Hybrid Model Predictive Control of DC–DC Boost Converters With Constant Power Load

Zeinab Karami, *Student Member, IEEE*, Qobad Shafiee, *Senior Member, IEEE*, Subham Sahoo, *Member, IEEE*, Meysam Yaribeygi, Hassan Bevrani, *Senior Member, IEEE*, and Tomislav Dragicevic, *Senior Member, IEEE*

***Abstract*—This article presents a hybrid model predictive controller to ensure dc microgrid stability and enhance the performance of dc-dc boost converters interfaced with constant power loads (CPLs) in a hybrid system. Hybrid systems are dynamic systems with both continuous current mode and discontinuous current mode states. The main purpose in this article is to develop an advanced control technique for voltage regulation and stabilization of the converters in the presence of CPLs due to serious stability concerns, without considering the accurate modelling information of the system. In this regard, an automatic model, considering different modes of operation induced by semiconductor switches in dc-dc boost converters and highly non-linear nature of CPL is employed to design the proposed control approach. The non-linear CPL connected directly to a dc-dc boost converter is utilized to define an optimal tracking control problem by minimizing a finite-prediction horizon cost function, which is known as a finite control set MPC. The proposed controller, which is implemented in both continuous and discontinuous current modes, accounts for the regulation of output voltage within the predefined range. The effectiveness of the proposed hybrid model predictive control is verified using a comparative evaluation with discrete-time averaged model predictive control, continuous control set MPC, and the conventional PI control under experimental conditions. The results authenticate an improved dynamic performance, which can be applied to practical dc microgrids with CPLs.**

***Index Terms*—Automatic model, constant power load, dc microgrid, dc-dc boost converter, hybrid model predictive control, optimal control.**

I. Introduction

MICROGRIDS (MGs) including renewable energy sources (RESs), energy storage systems (ESSs), and interfacing devices i.e., power electronic converters, can help to overcome power system capacity limitations, improve efficiency, reduce emissions, and manage the variability of renewable sources. Nowadays, increasing attention has been drawn to dc MGs, owing to their interesting features such as: 1) higher efficiency, 2) reduced conversion losses, and 3) no need for control of frequency, reactive power, and power quality, which are all considerable challenges in ac MGs [1], [2]. The dc MGs are proposed for power supply of applications with dc loads like home appliances, electric vehicles (EVs), naval ships, space crafts, submarines, telecom systems and rural areas. Multi terminal high-voltage dc grid and low-voltage dc MGs have been proposed for large-scale wind power transmission, and commercial facilities (e.g., data centers [3], isolated island [4], etc.).

A key component of a MG is the power electronic interface between a generator or an ESS, and the load. The most common interfaces used in dc MGs are dc-dc buck and boost converters. When power electronic converters are tightly regulated, they behave as constant power loads (CPLs) at the input terminals [5], [6]. The negative incremental impedance characteristic at the input terminals affects the system stability and complicates the situation from a control viewpoint [7], [8]. The effect of the CPLs becomes more significant when MG operates in islanded mode owing to reduced damping. Different solutions have been suggested in the literature to cope with this issue, i.e., negative impedance instability problem such as: 1) passive resistance damping, 2) load shedding, 3) placement of ESSs at dc bus, and 4) linear and non-linear control strategies [9], [10].

There are various control strategies for the voltage and current control, and stabilization in dc-dc converters such as proportional-integral (PI), fuzzy logic, sliding mode control (SMC), model predictive control (MPC), state-dependent Riccati equation (SDRE) control, and etc., [11], [12]. Linear controllers are the simplest control systems to achieve a regulated dc voltage in MGs [5]. Linear control methods consider the system stability only around an equilibrium point. These methods have already been proposed in [9], [10], [13] to stabilize dc systems with CPLs. In [14], a linear algorithm region of attraction (ROA) based on a semi-definite optimization is expressed to simplify the analysis of stability in dc MGs. A series of modern linear control methods is presented in [15] to manage the negative incremental impedance of the load and time delay while delivering the load power. A dc-dc boost converter allows boosting the input voltage to a higher level using high-frequency switching. This converter has a major role as a power electronic interface in dc MGs e.g.,

Manuscript received February 2, 2020; revised July 16, 2020 and November 5, 2020; accepted December 19, 2020. Date of publication December 28, 2020; date of current version May 21, 2021. Paper no. TEC-00 121-2020. *(Corresponding author: Qobad Shafiee.)*

Zeinab Karami, Qobad Shafiee, and Hassan Bevrani are with the Smart/Micro Grids Research Center, Department of Electrical Engineering, University of Kurdistan, Sanandaj, P.C 66177-15175, Iran (e-mail: zeinab.karami@eng.uok.ac.ir; q.shafiee@uok.ac.ir; bevrani@uok.ac.ir).

Subham Sahoo is with the Department of Energy Technology, Aalborg University, Aalborg 9100, Denmark (e-mail: sssa@et.aau.dk).

Meysam Yaribeygi is with the EE Department, K. N. Toosi University of Technology, Tehran, P.C 19 697 64 499, Iran (e-mail: yaribeygi@email.kntu.ac.ir).

Tomislav Dragicevic is with the Department of Electrical Engineering, Technical University of Denmark, Copenhagen 2800, Denmark (e-mail: tomdr@elektro.dtu.dk).

Color versions of one or more figures in this article are available at https://doi.org/10.1109/TEC.2020.3047754.

Digital Object Identifier 10.1109/TEC.2020.3047754

0885-8969 © 2020 IEEE. Personal use is permitted, but republication/redistribution requires IEEE permission.
See https://www.ieee.org/publications/rights/index.html for more information.

Authorized licensed use limited to: East Carolina University. Downloaded on June 18,2021 at 00:44:42 UTC from IEEE Xplore. Restrictions apply.

for solar PV systems, ESSs and EVs [16], [17]. With the dc-dc converters being inherently non-linear, an integrated CPL further increases the degree of non-linearity of dc MGs. Therefore, classical linear control methods are challenged and faced with some stability limitations. To guarantee stability, a non-linear PI stabilizing controller has been proposed in [18]. Variable switching frequency is the main problem of this method because of a negative impact on the converter efficiency and the design of the output filters [19]. Furthermore, PI tuning is frequently necessary for each perturbation due to the high variability and stochastic nature of solar energy in MGs which leads to the increased complexity of the system. In addition to the major problem associated with the PI controller, it is the fact that PI is a linear controller while all power electronics systems are mostly nonlinear and also the CPLs imposes a destabilizing nonlinear impact on the dc power electronic converters by an inverse voltage which results in remarkable fluctuations in the voltage term of the main bus. Therefore, tuning this type of linear controllers are being complicated. The authors in [8] present a non-linear sliding-mode control to develop a control law guaranteeing an enlarged region of local stability along with improved large-signal stability. The main disadvantage of SMC is that it is difficult to impose constraints or to regulate abstract quantities.

Recently, MPC methods are employed for direct control modulation of converters by optimizing a user-defined performance index due to its significant advantages over conventional control methods, such as fast dynamic response, simple handling of multi-variable systems, and taking account nonlinearity dynamic, uncertainty, and constraints [20]–[23]. In power electronics, the MPC can be divided into continuous control set MPC (CCS-MPC) and finite control set MPC (FCS-MPC). The CCS-MPC uses the pulse-width modulation (PWM) or space vector modulation (SVM) modulators to separate the switching frequency from the controller sampling time, thus converters operate in constant switching frequency which is more usable in industrial applications. On the other hand, the FCS-MPC does not need a modulator and has a variable switching frequency, and usually yields a good transient performance than CCS-MPC. Most especially, in power electronics more utilize FCS-MPC with a complete enumeration method to get prediction and optimization due to the nature of power converters that are combination of finite switching states [24]. A FCS-MPC algorithm to solve the unstable dynamic interactions between a CPL and a dc microgrid is given in [21]. Furthermore, a CCS-MPC is proposed to improve the inner current loop control performance in [22]. A constrained direct voltage FCS-MPC method, consisting of bounded currents and voltages of system for control of buck-boost converters is provided in [23].

In this paper, the above mentioned non-linear behavior of the system is taken into account using averaged and automatic models. The objective is to provide a formidable control strategy for dc-dc boost converters considering the CPL. Thus, an optimal controller based on hybrid model predictive controller (HMPC) technique is studied and compared with discrete-time averaged model predictive control (DTA-MPC) [25], and PI controller. The HMPC approach provides a systematic design procedure to guarantee good performance within the constraints. This proposed method utilizes a discrete automatic model in the prediction and design procedure, taking into account all switching modes to guarantees the system stability and noise-resilient. On the other hand, it overcomes the aforementioned drawbacks among different linear dynamics, logical transitions between continuous current mode (CCM) and discontinuous current mode (DCM) states, and other complex logical constraints, which needs to be considered in the system's variables. Finally, to further emphasize the good performance of the proposed controller, the results of this controller are compared with the CCS-MPC against a load change. The contribution of the present work and the novelty of the proposed controller can be summarized as follows:

- An HMPC control is proposed to provide an optimal switching of dc-dc converters at each step-time. The aim of the proposed control method is to guarantee the stability and sensitivity as well as produce accurate voltage and current under existing disturbances, such as faults and highly variable power generation and load demand. The unknown disturbances is considered as Additive White Gaussian Noise (AWGN), which the proposed solution can easily address inherent those fluctuations and uncertainties in the system.
- An augmented model is introduced by considering all operation modes of controlled switch and inductor current. This model is provided to obtain integral modes, which causes eliminate of disturbances and achieves tracking of signals error in both transient and steady-state stages, as well as ensuring the stability improvement and noise-free.
- The proposed controller takes the duty of inner loops such as current/voltage of dc MGs using a single optimal controller loop, with taken into account two-term to penalize deviation from the desired trajectory of both inner loops in the objective function.

The rest of this paper is organized as follows. In Section II, averaged and automatic models for dc-dc boost converters integrated with the CPL are discussed in detail. The implementation of proposed control strategy is introduced in Section III. The verification of the stability and sensitivity analysis in presence of HMPC is presented in IV. In Section V, experimental studies are provided, and finally, Section VI concludes the paper.

II. Modelling and Analysis

The schematic diagram of a dc-dc boost converter with a CPL is shown in Fig. 1. In the equivalent circuit, distributed generation (DG) is represented by a constant voltage source with input voltage V_{in}. The output voltage over the CPL is considered as well as voltage V_{C_o} across the output capacitor filter C_o. R_L is internal resistance of input inductor L and C_o, P is load power, S and D are two power switches; where S is controllable (MOSFET or IGBT), whereas D is uncontrollable. The converter operates in CCM, where the inductor current is always greater than zero in the averaged model, while it is greater than or equal to zero in the automatic model. Details of the continuous-time model of the proposed system in averaged

Authorized licensed use limited to: East Carolina University. Downloaded on June 18,2021 at 00:44:42 UTC from IEEE Xplore. Restrictions apply.

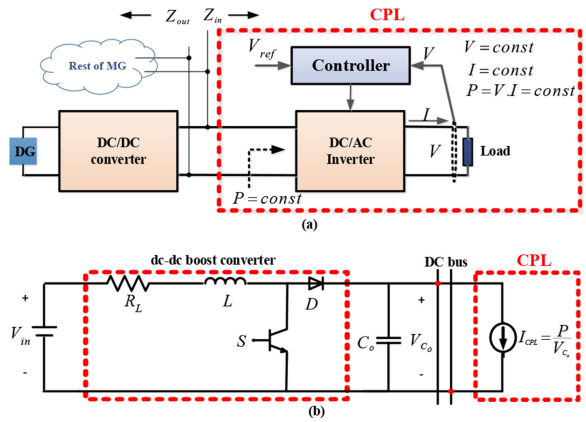

Fig. 1. Schematic diagram of a dc-dc boost converter with a CPL: (a) real circuit of system, (b) equivalent circuit of the system.

and automatic models presented in [26], the summary of these models are provided in the following subsections.

A. Averaged Continuous Time Model

There are two different dynamics corresponding to the switch positions in dc-dc boost converter for an averaged model [25].

Taking into account the switching modes, the following non-linear state-space representation describes the dynamics of the system based on an averaged model that can be given by:

$$\dot{x}(t) = \begin{cases} A_1 x(t) + Bu(t) & S = 1 \\ A_2 x(t) + Bu(t) & S = 0 \end{cases}$$
$$y(t) = Cx(t) \tag{1}$$

B. Automatic Continuous Time Model

Similar to the averaged model explained in Section II-A, the switching modes have been also considered for an automatic model. The only difference is that the inductor current discharge condition is considered in each sampling time. This difference creates a system with CCM and DCM states (i.e., the hybrid system). Three different dynamics are associated with the switch positions for the boost converter in the automatic model [26].

The automatic model can be calculated as follows:

$$\dot{x}(t) = \begin{cases} A_1 x(t) + Bu(t) & S = 1 \ \& \ i_L(t) > 0 \\ A_2 x(t) + Bu(t) & S = 0 \ \& \ i_L(t) > 0 \\ A_3 x(t) & S = 0 \ \& \ i_L(t) = 0 \end{cases}$$
$$y(t) = Cx(t) \tag{2}$$

where, $x(t) = [i_L(t)\ V_{C_o}(t)]^T$ is defined as the state vector including inductor current $i_L(t)$ and capacitor voltage $V_{C_o}(t)$, $u(t) = V_{in}(t)$ is input voltage, $y(t)$ is the output of the system which is the output voltage, and matrices A_1, A_2, A_3, B, and C are calculated as follows:

$$A_1 = \begin{bmatrix} \frac{-R_L}{L} & 0 \\ 0 & \frac{-P}{C_o V_{C_o}^2} \end{bmatrix}, A_2 = \begin{bmatrix} \frac{-R_L}{L} & \frac{-1}{L} \\ \frac{1}{C_o} & \frac{-P}{C_o V_{C_o}^2} \end{bmatrix},$$
$$A_3 = \begin{bmatrix} 0 & 0 \\ 0 & \frac{-P}{C_o V_{C_o}^2} \end{bmatrix}, B = \begin{bmatrix} \frac{1}{L} & 0 \end{bmatrix}^T, C = [0\ 1] \tag{3}$$

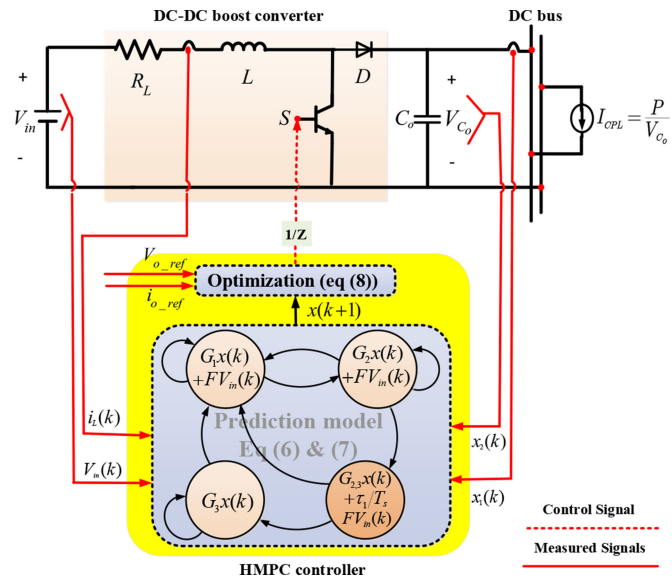

Fig. 2. Schematic of the closed-loop system with the proposed HMPC controller.

III. Proposed Control Strategy

Different modes of operation and several constraints (on the duty cycle and the inductor current) are applied on the power semiconductor switches. The dc-dc converters pose challenging hybrid control problems. To deal with above-mentioned challenges, this paper proposes an HMPC control strategy. The main objective of the proposed control scheme is to derive an optimal switching strategy such that the output voltage can be regulated along its reference trajectory. Fig. 2 shows a general scheme of the proposed HMPC controller applied to the system. The overall design steps of this control framework are:

1) Obtaining the discrete-time model of the system
2) Defining the cost function
3) Optimization problem

In order to implement the proposed HMPC, the following steps are carried out:

1) The optimal control action $u^*(k)$ is considered at $k-1$ instant and is applied to the dc-dc boost converter, (for every switching period k, the duty cycle $u^*(k) \in \{0, 1\}$ is chosen by the controller).
2) The current i_k and the capacitor voltage V_{C_o} are measured at k instant, and the references current i_{L_ref} and voltage V_{o_ref} are defined.
3) The prediction model of the system for the same instant is derived to predict the current and voltage values $i_L^p(k+1)$ and $V_{C_o}^p(k+1)$.
4) A cost function is evaluated using the reference current and voltage, as well as the prediction inductor current and capacitor voltage.

The proposed control objective is to achieve accurate output power by ensuring tight regulation of output voltage and current. Moreover, constraints can be imposed on the state variables and/or the manipulated variables, i.e., the control inputs. The underlying optimization problem is solved in real-time at each

Authorized licensed use limited to: East Carolina University. Downloaded on June 18,2021 at 00:44:42 UTC from IEEE Xplore. Restrictions apply.

time step to determine the plan of control actions over a finite prediction horizon. The sequence of control inputs that minimize the objective function leads to an optimal solution. In this sequence, only the first input is applied to the system. In the next time step, the planning process is repeated with updated measurements or estimation, while the time horizon is shifted one step forward. To do this, dc-dc boost converters have been described using a hybrid dynamical model where both continuous and discontinuous components are considered. Considering such dynamics, the HMPC could be an appropriate control strategy to guarantee the above-mentioned objectives.

A. Implementation of the Proposed Control Strategy

Due to the usage of intensive power electronics interfaces in dc MGs, the stability of such systems when connected to CPLs is a challenge. Hence, an HMPC approach is proposed to solve the instability problem and to regulate the output voltage of dc-dc boost converters with CPL. The control objective is to determine optimal switching of the system in a hybrid optimal control methodology, such that the output voltage is regulated according to its reference trajectory under different scenarios. Details are described in the following three steps:

Step 1: Determining of discrete-time model.

The continuous-time equations of both two models as given in (1) and (2) are discretized using the Euler approximation approach as:

$$\frac{dx(t)}{dt} = \frac{x(k+1) - x(k)}{T_s} \tag{4}$$

Accordingly, the averaged and automatic discrete-time models of the studied system with one unit and the CPL can be written in (5), (6) and (7), respectively.

$$\begin{aligned} x(k+1) &= (S)\left(E_1 x(k) + Fu\right) + (1-S)\left(E_2 x(k) + Fu\right) \\ y(k+1) &= Hx(k) \end{aligned} \tag{5}$$

$$\begin{aligned} x(k+1) &= \begin{cases} G_1 x(k) + FV_{in}(k) & S = 1 \\ G_2 x(k) + FV_{in}(k) & S = 0 \;\&\; i_L(k+1) > 0 \\ G_3 x(k) & S = 0 \;\&\; i_L(k+1) = 0 \end{cases} \\ y(k+1) &= Hx(k) \end{aligned} \tag{6}$$

where $E_1 = I + A_1 T_s$, $E_2 = I + A_2 T_s$, $G_1 = I + A_1 T_s$, $G_2 = I + A_2 T_s$, and $G_3 = I + A_3 T_s$. Furthermore, I is the identity matrix, $F = BT_s$, $H = C$, and T_s is the sampling time. After discretization, the automatic model can operate in four different modes.

Fig. 3 illustrates different modes of duty cycle and the inductor current where the red line represents switched OFF and ON stages of the controllable switch, and the dashed line represents the inductor current changes. Taking into account the status of inductor current and the switch, there will be four different modes after discretization.

Mode 1: When the inductor current is positive and the switch is ON for the whole sampling interval, i.e., $S = 1$, $i_L(k) > 0$, and $i_L(k+1) > 0$.

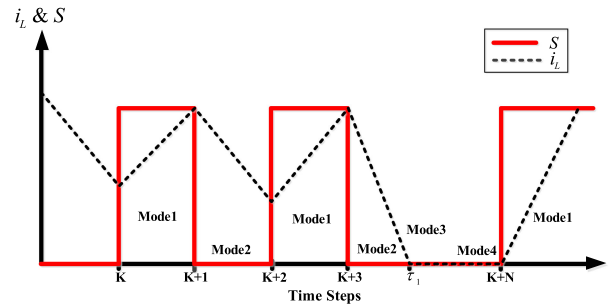

Fig. 3. Operation modes of the boost converter after discretization.

Mode 2: When the inductor current is positive and the switch is OFF for the whole sampling interval, i.e., $S = 0$, $i_L(k) > 0$, and $i_L(k+1) > 0$.

Mode 3: When the inductor current reaches zero during the sampling interval, while the switch is OFF, i.e., $S = 0$, $i_{Li}(k) > 0$, and $i_{Li}(k+1) = 0$.

Mode 4: When the inductor current is zero and the switch is OFF for the whole sampling interval i.e., $S = 0$, and $i_L(k) = i_L(k+1) = 0$.

It should be noted that an additional operational mode (mode 3) is added to the continuous automatic model in discrete time domain. Thus, the following equation can be added to the discrete-time equations of the automated model.

$$x(k+1) = G_{2,3}x(k) + \frac{\tau_1}{T_s} FV_{in}(k) \tag{7}$$

where $G_{2,3} = (1/T_s)(\tau_1 G_2 + \tau_2 G_3)$, $T_s = \tau_1 + \tau_2$ and τ_1 denotes the time instant within the sampling interval, when the inductor current reaches zero, i.e., $i_L(k + \frac{\tau_1}{T_s}) = 0$. Fig. 4 in [26] illustrates mode transitions for both CCM and DCM modes when switch position and the inductor current change in automatic model. The discrete-time automatic model is utilized in the proposed controller in order to achieve an improved performance.

Step 2: Defining the cost function.

The cost function is formulated based on the control objective. Since the main objective of the proposed control design is to ensure output power of load, so that the output voltage and the output current track the reference values. In this regard, the error between the predicted value of the variables and the desired variables values as well as the variation of control signals over the prediction horizon is taken into consideration for performance index of the HMPC, i.e.,

$$J(k) = \frac{1}{N_p}\left\{\sum_{k=1}^{N_p} \left|P_{o_ref} - P_o^p(k+1)\right| + \lambda\left|\Delta u(k)\right|\right\} \tag{8}$$

where N_p is the prediction horizon, P_{o_ref} and $P_o^p(k+1)$ are output power reference and prediction, which are equal to $P_{o_ref} = i_{o_ref} * V_{o_ref}$ and $P_o^p(k+1) = i_o^p(k+1) * v_{C_o}^p(k+1)$ respectively. Moreover, V_{o_ref} is equal to V_{dc}^*, $V_{C_o}^p$ is capacitor voltage prediction and

Authorized licensed use limited to: East Carolina University. Downloaded on June 18,2021 at 00:44:42 UTC from IEEE Xplore. Restrictions apply.

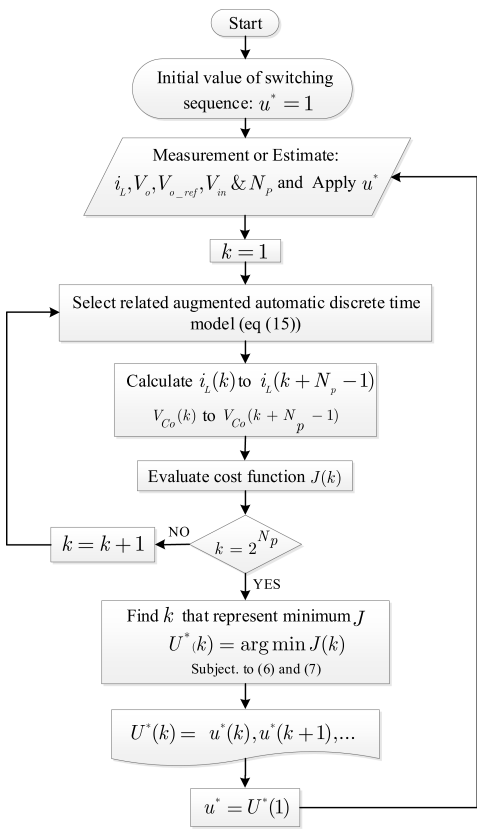

Fig. 4. Flowchart of the HMPC controller.

i_o can be achieved by applying kirchoff's current law (KCL) as:

$$i_o = i_L - i_C$$
$$\Rightarrow \begin{cases} i_{o_ref}(k+1) = i_{L_ref}(k+1) - i_{C_ref}(k+1) \\ i_o^p(k+1) = i_L^p(k+1) - i_C^p(k+1) \end{cases} \quad (9)$$

where $i_C = C\frac{dV_{Co}}{dt}$, consequencely i_{C_ref} and i_C^p based on the Euler approximation approach can be calculated as:

$$i_{C_ref}(k+1) = C\frac{V_{dc}(k+1) - V_{dc}(k)}{T_s}$$
$$i_C^p(k+1) = C\frac{V_{C_o}^p(k+1) - V_{C_o}^p(k)}{T_s} \quad (10)$$

It is worth notifying that $V_{dc}(k)$ is a probability value of the dc bus voltage that may be higher or lower than the rated dc voltage V_{dc}^*, and $V_{dc}(k)$ will reach to V_{dc}^* in N_p steps taking into account the next instant $(k+1)$. The dc bus voltage can be obtained as follows [27]:

$$V_{dc}(k+1) = V_{dc}(k) + \frac{1}{N_p}(V_{dc}^* - V_{dc}(k)) \quad (11)$$

Further, i_L^p and i_{L_ref} are inductor current prediction and references, where i_{L_ref} can be achieved using the power balance equation $P_{in} = P_{out}$ and the desired current can be calculated as:

$$P_{in} = V_{in}i_L,\ P_{out} = P_{Load} \quad \Rightarrow i_{L_des} = \frac{P_{Load}}{V_{in}} \quad (12)$$

where P_{in}, P_{out} and P_{Load} are input power, output power, and load power respectively. To improve the transient response of the output voltage, a term proportional to the voltage error, i.e., $V_{o_ref} - V_o$ is added to the above equation, i.e.

$$i_{L_ref} = i_{L_des} + h\,(V_{o_ref} - V_o) \quad (13)$$

where $h \in \mathcal{R}^+$ is the small-ripple approximation for regulation of output voltage in steady-state.

Further, $\Delta u(k)$ is an error between two consecutive switching states $u(k) - u(k-1)$ calculated by the proposed HMPC controller, and $\lambda > 0$ is the weighting factor which sets the trade-off between the inductor current/output voltage error and the switching frequency. Some guidelines for tuning the weighting factor are provided in [28].

Step 3: Formulation of optimization problem.

At each time sample, state variables are measured or estimated to minimize the given cost function using the below optimization problem:

$$U^*(k) = \arg\min J(k)$$
$$\text{subject to (6)} - \text{(7)} \quad (14)$$

Minimizing the above-mentioned cost function results in a sequence in the form U^*, where $U^*(k) = \{u^*(k), u^*(k+1), \ldots\}$. There exist 2^{N_p} switching sequences and only its first element i.e., $u^*(k)$ is applied in each sampling time and is shifted the prediction horizon one step forward. The details of the proposed controller implementation is provided in Fig. 4.

IV. Stability Analysis

As mentioned earlier, when the CPLs are integrated into the dc bus of the dc MG, the stability improvement becomes important issue since the negative impedance characteristic of the CPL may cause the system instability and complicate the solution from control point of view. Therefore, performance of the system in the presence of the proposed controller should be satisfied and sustainable with small overshoot, fewer oscillations, and smooth transient performance.

A. Stability Analysis for the Open-Loop System

The stability assessment for the open-loop system in (2), which is the completed model of the system due to considering all switching modes and inductor current conditions, is presented by the equilibrium points: $\alpha = (0.023, 12\,030)$, $\beta = (1.5199.98)$, and $\gamma = (0, \infty)$. These points are obtained using $\dot{x}(t) = 0$ in equation (2). Since α and γ are always unstable, and the system is a second-order, to investigate the stability analysis around β, the phase plane method can be used. Fig. 5 demonstrates the phase plane stability analysis of the system around this point. As shown in Fig. 5, β is an unstable equilibrium due to all trajectories in the vicinity of the limit cycle diverge from it as $t \to \infty$. Hence, the open-loop system is unstable.

B. Stability Analysis of the Closed-Loop System

The stability analysis of the closed-loop system can be defined by examining Lyapunov theory taking account the accurate

Authorized licensed use limited to: East Carolina University. Downloaded on June 18,2021 at 00:44:42 UTC from IEEE Xplore. Restrictions apply.

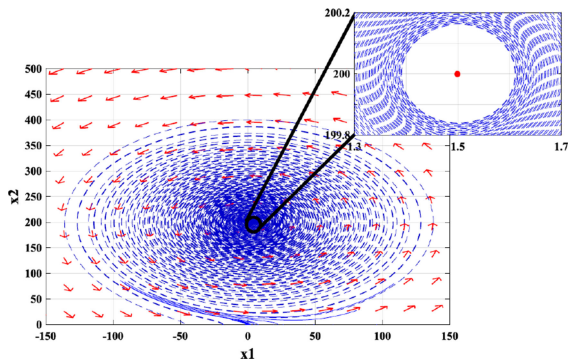

Fig. 5. The phase plane analysis of the opened-loop system.

nonlinear dynamic model and all switching modes of the dc-dc boost converter. The complete state-space model used for the HMPC system design is described in (6) and (7). To confirm the stability enhancement of the proposed HMPC control, a detailed stability analysis is presented. In this regard, the augmented automatic discrete-time model of the system taking into account all switching modes and the inductor current situations is provided as follows [26]:

$$X(k+1) = \begin{cases} \overline{\mathrm{G}}_1 X(k) + \overline{\mathrm{F}}\Delta v_{si}(k), \\ \overline{\mathrm{G}}_2 X(k) + \overline{\mathrm{F}}\Delta v_{si}(k), \\ \overline{\mathrm{G}}_3 X(k), \\ \overline{\mathrm{G}}_4 X(k) + \frac{\tau_1}{T_s}\overline{\mathrm{F}}\Delta v_{si}(k) \end{cases}$$

$$Y(k) = \overline{\mathrm{H}} X(k) \tag{15}$$

where Δx, and $\Delta v_{si}(k)$ are differences of the states, and the input vectors respectively, and matrices $X(k)$, $\overline{\mathrm{G}}_m$, $\overline{\mathrm{F}}$, and $\overline{\mathrm{H}}$ and Y are calculated as follows:

$$X(k) = \left[\Delta x(k)\ y(k)\right]^T, \overline{\mathrm{G}}_m = \begin{bmatrix} G_m & O^T \\ HG_m & I_{q\times q} \end{bmatrix}$$

$$\overline{\mathrm{F}} = \left[F\ HF\right]^T, \overline{\mathrm{H}} = \left[0\ I_{q\times q}\right]$$

In matrix $\overline{\mathrm{G}}_m$, $m = 1, \ldots, 4$ which represents different modes and O^T is zero vector with appropriate dimension $(q \times n)$ that n is the dimension of the state variable vector, and q is the number of outputs, that q integrators are embedded in the augmented model.

$$Y = \left[y\left(k_i+1|k_i\right) \cdots y\left(k_i+N_p k_i\right)\right]^T = \Gamma X\left(k_i\right) + \Phi\Delta U$$

where, $\Gamma = [\overline{\mathrm{HG_m}}\ \overline{\mathrm{HG_m}}^2 \cdots \overline{\mathrm{HG_m}}^{N_p}]^T$, and

$$\Phi = \begin{bmatrix} \overline{HF} & 0 & \ldots & 0 \\ \overline{HGF} & \overline{HF} & \ldots & 0 \\ \overline{HG}^2\overline{F} & \overline{HG_mF} & \ldots & 0 \\ \vdots & & & \\ \overline{HG}^{N_p-1}\overline{F} & \overline{HG}^{N_p-2}\overline{F} & \ldots & \overline{HG}^{N_p-N_c}\overline{F} \end{bmatrix}$$

$\Delta U(k)$, through minimizing the given objective function is obtained as:

$$\Delta U = \left(\Phi^T\Phi + R\right)^{-1}\Phi^T\left(R_s - \Gamma X\left(k_i\right)\right) \tag{16}$$

where, $R = (r_w)I_{N_c\times N_c}$ is a diagonal matrix in which $r_w \geq 0$ and is used as a tuning parameter, N_c is the control horizon such that its value is selected to be less than or equal to prediction horizon (N_p), $R_s^T = \overbrace{[1\ 1 \ldots 1]}^{N_p} r(k_i)$, and $r(k_i)$ is set-point signal. Due to the receding principle of horizon control, only the first element of the control signal is applied in each sample time as the control signal, thus

$$\begin{aligned} \Delta u\left(k_i\right) &= \overbrace{[1\ 0 \cdots 0]}^{N_c}\left(\Phi^T\Phi + R\right)^{-1}\left(\Phi^T R_s r\left(k_i\right)\right. \\ &\quad \left. - \Phi^T\Gamma X\left(k_i\right)\right) \\ &= K_y r\left(k_i\right) - K_{mpc} X\left(k_i\right) \end{aligned} \tag{17}$$

where, K_y and K_{mpc} are state feedback control gain related to y and feedback control gain using MPC respectively. Finally, by substituting (17) in (15), the closed-loop state-space equation of the system can be written as:

$$\begin{aligned} X(k+1) &= \overline{\mathrm{G_m}}X(k) - \overline{\mathrm{F}}K_{mpc}X(k) + \overline{\mathrm{F}}K_y r(k) \\ &= \left(\overline{\mathrm{G}} - \overline{\mathrm{F}}K_{mpc}\right)X(k) + \overline{\mathrm{F}}K_y r(k) \end{aligned} \tag{18}$$

The closed-loop system under the MPC scheme is asymptotically stable if there exists [29]:

1) $V(x) \geq 0$ for all x and $V(0) = 0$,
2) $\Delta V(x) = V(f(x)) - V(x)$ for all x.

The Lyapunov function candidate to investigate the stability improvement of the closed-loop system due to the nonlinear dynamics of the augmented automatic model is introduced as follows:

$$V(X(k)) = X^2(k) \tag{19}$$

$$\begin{aligned} \Delta V(X(k)) &= (A_{close}X(K) + B_{close}r(k))^2 - X^2(k) \\ &\simeq -(I - A_{close}^2)X^2(k) + (B_{close})^2(r(k))^2 \leq 0 \end{aligned} \tag{20}$$

where $A_{close} = (\overline{\mathrm{G_m}}X(k) - \overline{\mathrm{F}}K_{mpc}i)$, $B_{close} = \overline{\mathrm{F}}K_y r(k)$. Given that the $(I - A_{close}^2)$ is positive definite and invertible then,

$$\Delta V(X(k)) \leq -(I - A_{close}^2)X^2(k) + (B_{close})^2(r(k))^2 \tag{21}$$

Thus,

$$\Delta V(X(k)) \leq 0, \forall X^2(k) \geqslant (I - A_{close}^2)^{-1}(B_{close})^2(r(k))^2 \tag{22}$$

by substituting the value of A_{close} and B_{close}, (22) means that the closed-loop system (18) is stable with respect to constant and positive $r(k)$.

In addition, a comparison of the sensitivity and stability improvement of the closed-loop system in the presence of different controllers to confirm the improvement in performance and guarantee the robustness of the closed-loop system in the presence of the proposed controller for various values of C_o and P are shown in Figs. 6 and 7, respectively. In order to evaluate and compare the performance of sustainability, a conventional

Authorized licensed use limited to: East Carolina University. Downloaded on June 18,2021 at 00:44:42 UTC from IEEE Xplore. Restrictions apply.

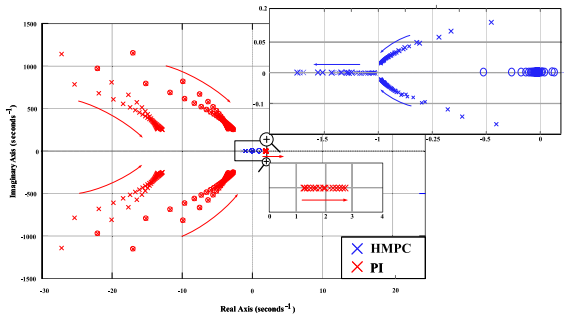

Fig. 6. The trajectory of the system's eigenvalues against various values of C_o and P.

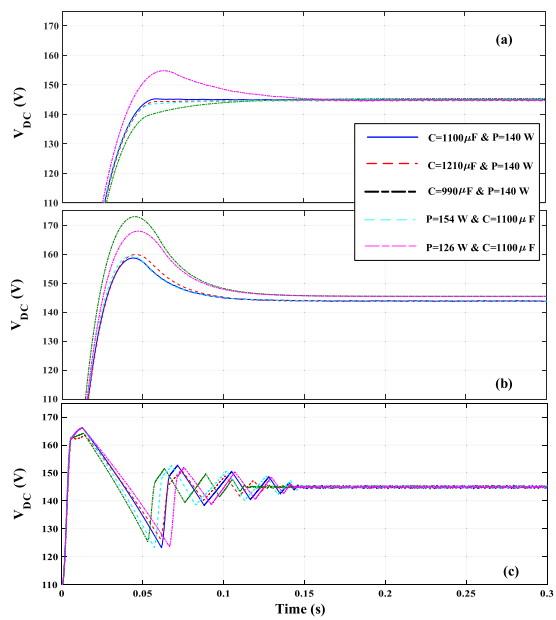

Fig. 7. Sensitivity analysis of the designed controllers for $\pm 10\%$ change in capacitance and power load: (a) HMPC, (b) DTA-MPC, and (c) PI.

technique for stability improvement like root locus is used. Fig. 6 shows the trajectory of the closed-loop system's eigenvalues against the change in parameters. It can be seen from Fig. 6, that the trajectory of the roots of the closed-loop system through the proposed controller for the entire range of the parametric changes lies well within the left half of the S-plane resulting a stable control loop, while for the PI controller, the eigenvalues of the closed-loop system with the variation of parameters move toward the right side of the S-plane which leading to unstable regions.

Also, a comprehensive sensitivity analysis of the closed-loop system with various controllers under parametric uncertainties is illustrates in Fig. 7. The effectiveness and the performance robustness of the proposed controller rather than other controllers are verified under $\pm 10\%$ variation in output capacitor filter (C_o) and power load (P). In other words, the lack of significant difference in the settling time ensures that the proposed algorithm is robust to parameter uncertainties.

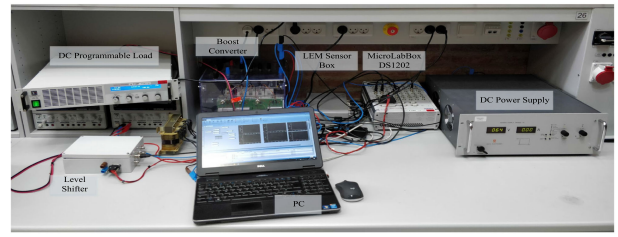

Fig. 8. Experimental dc setup.

TABLE I
ELECTRICAL AND CONTROL PARAMETERS

Electrical Parameters		
Parameter	Symbol	Value
The dimension of the state variable vector	n	2
The number of outputs	q	1
Input voltage	V_{in}	110 V
Voltage reference	V_{dc}^*	145 V
CPL	P	140 W
Filter inductance	L	1860 μH
Filter capacitance	C_o	1100 μF
Input resistance	R_i	0.01 Ω
Control Parameters		
Sampling time	T_s	0.1 ms
Prediction horizon	N_p	3
Weighting factor	λ	0.01
Ripple approximation	h	0.7

V. EXPERIMENTAL RESULTS

A complete model of dc-dc boost converter based on switching operation modes and inductor current (see Fig. 4 in [26]) is considered. The performance of the proposed HMPC is evaluated for one distributed generation unit (DGU) of an islanded dc MG system as shown in Fig. 2, including a programmable dc source for supporting a CPL interfaced with a dc-dc boost converter. The experimental prototype DC setup is shown in Fig. 8. The dc-dc boost converter is supplied by a dc power supply. The current and the voltage are measured with a LEM sensor box. The dSPACE MicroLabBox DS1202 is used to implement the control framework on the prototyped system. The electrical and control parameters of the test system are listed in Table I. In order to validate the proposed control framework, the provided results of the controller using automatic model are compared with the DTA-MPC, the CCS-MPC, and PI controller considering the following scenarios.

A. *Case Study 1: Load Step Change*

Fig. 9 shows performance of the proposed HMPC based on automatic model under CPL step change to evaluat convergence property of the applied control method. In order to validate the proposed control framework, the load is increased (the CPL changes by 37% from 140 W to 192 W at $t = 1.5$ s). The voltage regulation is shown in Fig. 9(a). As shown in Fig. 9, in the controller designed by the automatic model, dc voltage dips down to a lower value upon load change and returns to its initial value quickly, while in DTA-MPC based on the averaged model, the voltage does not return to its initial value. Additionally, it can be seen that the voltage regulation is well maintained using

Authorized licensed use limited to: East Carolina University. Downloaded on June 18,2021 at 00:44:42 UTC from IEEE Xplore. Restrictions apply.

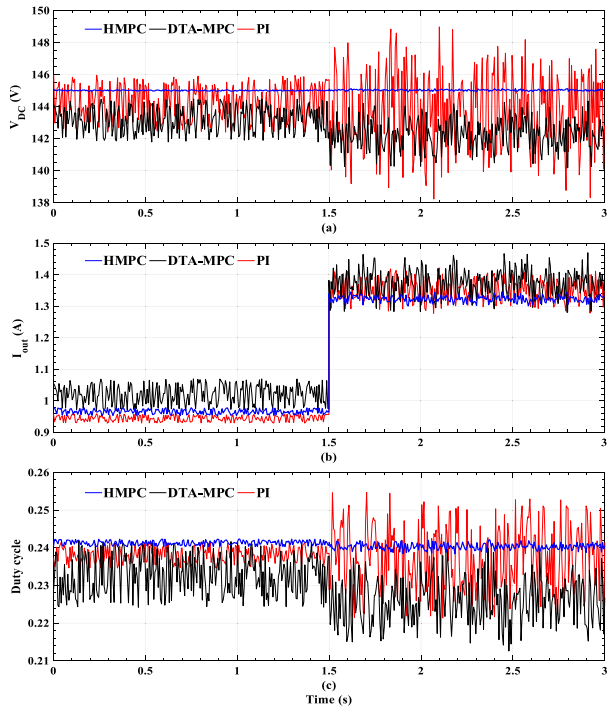

Fig. 9. Performance of the proposed HMPC controller under load step change: (a) output voltage, (b) load current, and (c) duty cycle.

the proposed HMPC controller compared with DTA-MPC, and PI controller, with very little variation instances in the desired range.

Figs. 9(b) and 10(c) show that current and duty cycle where dc voltage regulation convergence are achieved in HMPC, while DTA-MPC and the PI controllers are associated with most variation.

B. Case Study 2: Noise-Resilient Primary Voltage Control

From a practical point of view, the noise and microgrid configuration parameters are unknown, so it is necessary to consider the distributed dynamics, noises and uncertainties in the model design. One of the most important unmodelled and unknown disturbances in the primary layer of microgrids is sudden fluctuations in renewable energy sources (e.g. PVs and wind turbines (WTs), etc.) due to their high variability and stochastic nature. These disturbances can be modelled as AWGN based on the following expression:

$$x(k+1) = G_i x(k) + F V_{in}(k) + W(k) \tag{23}$$

where $i = 1, 2, 3$ and $W(k)$ is AWGN with $\sigma^2 = 0.1$. Indeed the objective of this case study is to demonstrate the robustness of the proposed control strategy under sudden input voltage fluctuations due to climate changes. Given that climate changes have an effect on the power produced by the PV arrays, it is assumed that the input voltage varies randomly in every t = 0.3 s (see Fig. 10). The transient behavior during frequent changes of the input voltage is analyzed and the performance of the HMPC method based on the automatic model comparing the DTA-MPC and the conventional PI controllers is shown in

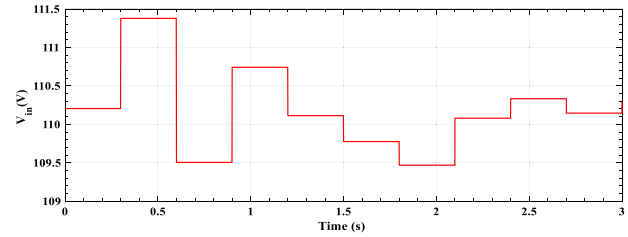

Fig. 10. Sudden input voltage variations.

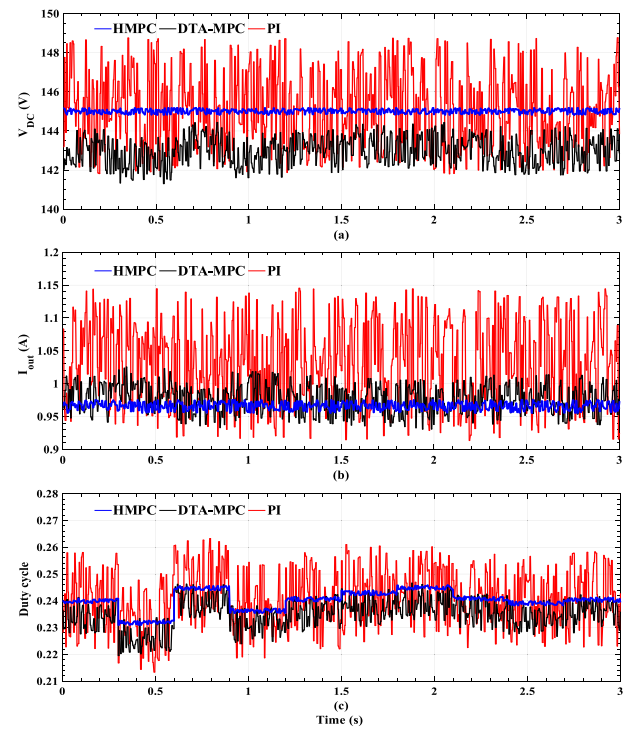

Fig. 11. Performance of the proposed HMPC controller under sudden input voltage variation: (a) output voltage, (b) output current, and (c) duty cycle.

Fig. 11. Although the PI control method has many advantages like stability and decentralized architecture of primary voltage controllers, it does not provide robustness with respect to sudden input voltage functionality of PV for the dc MG system in the presence of CPL. Comparison between the dynamical responses of controllers shows that the proposed HMPC control strategy provides a smooth and fast transient response.

C. Case Study 3:Comparing HMPC With CCS-MPC

In this scenario, the effectiveness and robustness of the proposed controller is investigated under a load change in comparison with the CCS-MPC. It is assumed that a frequent load change is occurred, with the nominal value p=140, step changes in times 1, and 2, seconds. While HMPC provides a superior performance rather than the other two controllers for all the above two scenarios as shown in Figs. 9 and 12. The experimental results in Fig. 12 show that the proposed method provides a fast dynamic response, small ripple, and low sonic noise rather than CCS-MPC.

Authorized licensed use limited to: East Carolina University. Downloaded on June 18,2021 at 00:44:42 UTC from IEEE Xplore. Restrictions apply.

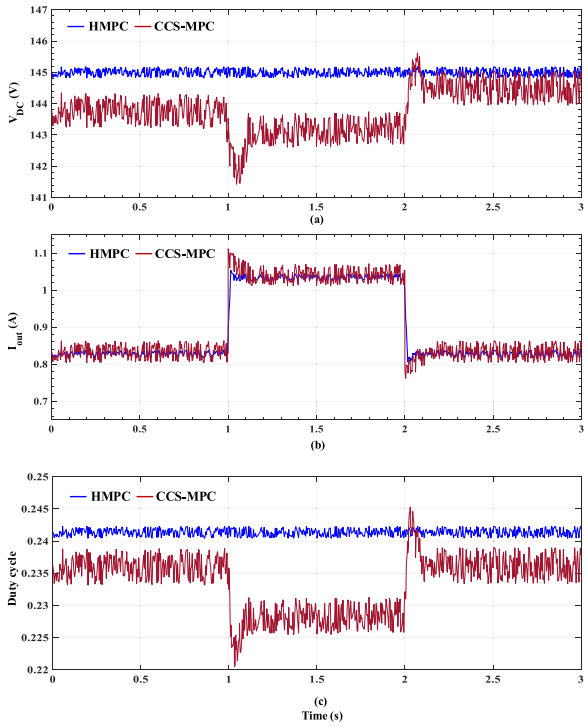

Fig. 12. Performance of the proposed HMPC controller compared under the frequent power load change of the CPL : (a) output voltage, (b) output current, and (c) duty cycle.

VI. Conclusion

This paper proposes a hybrid model predictive controller for dc-dc boost converters interfaced with CPLs based on two different modeling approaches: automatic and averaged. The proposed controller maintains stability of a highly non-linear system in the presence of CPLs while providing accurate output voltage tracking in different scenarios. Efficacy of the proposed solution under load change and variation of input voltage scenarios has been studied. Experimental results validate the effectiveness of the proposed HMPC method. The automatic model-based HMPC shows a superior performance comparing DTA-MPC and the conventional PI controllers. Furthermore, two strong candidates of MPC schemes are presented for dc bus voltage control of dc MG. Both FCS-MPC with optimal control and CCS-MPC are successfully implemented and investigated in order to adapt and to the frequent power load change of the CPL. It can be seen from the experimental results that although the two control methods exhibit good dynamic performance, the proposed controller which is as an FCS-MPC has a faster response with a minimum error and lower fluctuations.

References

[1] J. Chen, C. Wang, and J. Chen, "Investigation on the selection of electric power system architecture for future more electric aircraft," *IEEE Trans. Transp. Electrifi.*, vol. 4, no. 2, pp. 563–576, Jun. 2018.

[2] E. Skjong, R. Volden, E. Rodskar, M. Molinas, T. A. Johansen, and J. Cunningham, "Past, present, and future challenges of the marine vessel's electrical power system," *IEEE Trans. Transp. Electrifi.*, vol. 2, no. 4, pp. 522–537, Dec. 2016.

[3] T. Dragičević, X. Lu, J. C. Vasquez, and J. M. Guerrero, " microgrids-art: A review of control strategies and stabilization techniques," *IEEE Trans. Power Electron.*, vol. 31, no. 7, pp. 4876–4891, Jul. 2016.

[4] L. Xu and D. Chen, "Control and operation of a dc microgrid with variable generation and energy storage," *IEEE Trans. Power Delivery.*, vol. 26, no. 4, pp. 2513–2522, Oct. 2011.

[5] A. Kwasinski and C. N. Onwuchekwa, "Dynamic behavior and stabilization of dc microgrids with instantaneous constant-power loads," *IEEE Trans. Power Electron.*, vol. 26, no. 3, pp. 822–834, Mar. 2011.

[6] A. M. Rahimi and A. Emadi, "Active damping in dc/dc power electronic converters: A novel method to overcome the problems of constant power loads," *IEEE Trans. Ind. Electron.*, vol. 56, no. 5, pp. 1428–1439, May 2009.

[7] Q. Xu *et al.*, "Design and stability analysis for an autonomous dc microgrid with constant power load," in *Proc. IEEE Appl. Power Electron. Conf. Expo.*, May 2016, pp. 3409–3415.

[8] E. Hossain, R. Perez, A. Nasiri, and S. Padmanaban, "A comprehensive review on constant power loads compensation techniques," *IEEE Access*, vol. 6, pp. 33 285–33 305, Jun. 2018.

[9] M. Cespedes, L. Xing, and J. Sun, "Constant-power load system stabilization by passive damping," *IEEE Trans. Power Electron.*, vol. 26, no. 7, pp. 1832–1836, Jul. 2011.

[10] Z. Qu, S. Ebrahimi, N. Amiri, J. Jatskevich, and A. Pizniur, "Adaptive control method for stabilizing dc distribution systems with constant-power loads based on tunable active damping," in *Proc. IEEE 19th Workshop Control Model. Power Electron.*, Sep. 2018, pp. 1–6.

[11] T. Dragicevic, S. Vazquez, and P. Wheeler, "Advanced control methods for power converters in DG systems and microgrids," *IEEE Trans. Ind. Electron.*, to be published, doi: 10.1109/TIE.2020.2994857.

[12] Z. Karami, Q. Shafiee, Y. Batmani, and H. Bevrani, "On the design of suboptimal controller for dc microgrids with cpl," *Energy Procedia*, vol. 141, pp. 611–618, 2017.

[13] F. Gao *et al.*, "Comparative stability analysis of droop control approaches in voltage-source-converter-based dc microgrids," *IEEE Trans. Power Electron.*, vol. 32, no. 3, pp. 2395–2415, Mar. 2016.

[14] H. Ji, J. Sun, M. Huang, L. Wei, and X. Zha, "A nonlinear large-signal model for dc-dc converters," in *Proc. IEEE 8th Int. Power Electron. Motion Control Conf., IPEMC-ECCE Asia*, Jul. 2016, pp. 2183–2186.

[15] B. M. Grainger, Q. Zhang, G. F. Reed, and Z.-H. Mao, "Modern controller approaches for stabilizing constant power loads within a dc microgrid while considering system delays," in *Proc. IEEE 7th Int. Symp. Power Electron. Distrib. Gener. Syst.*, Aug. 2016, pp. 1–6.

[16] K. Liu, T. Liu, Z. Tang, and D. J. Hill, "Distributed mpc-based frequency control in networked microgrids with voltage constraints," IEEE Trans. Smart Grid., vol. 10, no. 6, pp. 6343–6354, Nov. 2019.

[17] M. K. Kazimierczuk, *Pulse-Width Modulated DC-DC Power Converters*, John Wiley & Sons, 2015.

[18] R. Tiwari, N. R. Babu, R. Arunkrishna, and P. Sanjeevikumar, "Comparison between pi controller and fuzzy logic-based control strategies for harmonic reduction in grid-integrated wind energy conversion system," in *Advances in Smart Grid and Renewable Energy*. Springer, 2018, pp. 297–306.

[19] H.-J. Yoo, T.-T. Nguyen, and H.-M. Kim, "MPC with constant switching frequency for inverter-based distributed generations in microgrid using gradient descent," *Energies*, vol. 12, no. 6, pp. 1156–1169, Mar. 2019.

[20] T. Kobaku, S. C. Patwardhan, and V. Agarwal, "Experimental evaluation of internal model control scheme on a dc-dc boost converter exhibiting nonminimum phase behavior," *IEEE Trans. Power Electron.*, vol. 32, no. 11, pp. 8880–8891, Nov. 2017.

[21] T. Dragičević, "Dynamic stabilization of dc microgrids with predictive control of point-of-load converters," *IEEE Trans. Power Electron.*, vol. 33, no. 12, pp. 10 872–10 884, Dec. 2018.

[22] P. E. Kakosimos, A. G. Kladas, and S. N. Manias, "Fast photovoltaic-system voltage-or current-oriented mppt employing a predictive digital current-controlled converter," *IEEE Trans. Ind. Electron.*, vol. 60, no. 12, pp. 5673–5685, Dec. 2012.

[23] T. Geyer, G. Papafotiou, R. Frasca, and M. Morari, "Constrained optimal control of the step-down dc-dc converter," *IEEE Trans. Power Electron.*, vol. 23, no. 5, pp. 2454–2464, Sep. 2008.

[24] A. A. Ahmed, B. K. Koh, and Y. I. Lee, "A comparison of finite control set and continuous control set model predictive control schemes for speed control of induction motors," *IEEE Trans. Ind. Informat.*, vol. 14, no. 4, pp. 1334–1346, Apr. 2018.

Authorized licensed use limited to: East Carolina University. Downloaded on June 18,2021 at 00:44:42 UTC from IEEE Xplore. Restrictions apply.

[25] Z. Karami, Q. Shafiee, and H. Bevrani, "Model predictive and sdre control of dc microgrids with constant power loads: A comparative study," in *Proc. Smart Grid Conf.*, 2018, pp. 1–6.
[26] Z. Karami, Q. Shafiee, Y. Khayat, M. Yaribeygi, T. Dragicevic, and H. Bevrani, "Decentralized model predictive control of dc microgrids with constant power load," *IEEE Trans. Emerg. Sel. Topics Power Electron.*, to be published, doi: 10.1109/JESTPE.2019.2957231.
[27] D. E. Quevedo, R. P. Aguilera, M. A. Perez, P. Cortés, and R. Lizana, "Model predictive control of an afe rectifier with dynamic references," *IEEE Trans. Power Electron.*, vol. 27, no. 7, pp. 3128–3136, Jul. 2012.
[28] P. Cortés *et al.*, "Guidelines for weighting factors design in model predictive control of power converters and drives," in *Proc. IEEE Int. Conf. Ind. Technol.*, May 2009, pp. 1–7.
[29] A. Iggidr and M. Bensoubaya, "Stability of Discrete-Time Systems: New Criteria and Applications to Control Problems," 1996.

Zeinab Karami (Student Member, IEEE) received the B.Sc. and M.Sc. degrees from the University of Kurdistan, Sanandaj, Iran, in 2015 and 2017, respectively. She is currently a Researcher with the Smart/Micro Grids Research Center, University of Kurdistan. Her main research interests include microgrid stability and control, model predictive, nonlinear, optimal and robust control for the application of power electronics in distributed systems, networked microgrids, and machine learning.

Qobad Shafiee (Senior Member, IEEE) received the Ph.D. degree in electrical engineering from the Department of Energy Technology, Aalborg University, Aalborg, Denmark, in 2014. He is currently an Assistant Professor, the Director of International Relations, and a Program Co-Leader of the Smart/Micro Grids Research Center, University of Kurdistan, Sanandaj, Iran, where he was a Lecturer from 2007 to 2011. In 2014, he was a Visiting Scholar with the Electrical Engineering Department, University of Texas at Arlington, Arlington, TX, USA. In 2015, he was a Postdoctoral Fellow with the Department of Energy Technology, Aalborg University. His current research interests include modeling, energy management, the control of power electronics-based systems and microgrids, and the model predictive and optimal control of modern power systems.

Subham Sahoo (Member, IEEE) received the B.Tech. degree in electrical and electronics engineering from the VSS University of Technology, Burla, India, in 2014 and the Ph.D. degree in electrical engineering from the Indian Institute of Technology (IIT), New Delhi, India, in 2018. In 2017, he was a Visiting Student with the Department of Electrical and Electronics Engineering, Cardiff University, Cardiff, U.K. Prior to completion of his Ph.D., he was a Research Fellow with the Department of Electrical and Computer Engineering, National University of Singapore, Singapore. He is currently a Postdoctoral Researcher with the Department of Energy Technology, Aalborg University, Aalborg, Denmark. His research interests include control and stability of microgrids, renewable energy integration, cyber-physical power electronic systems, and cyber security in power electronic systems. He was the recipient of the Indian National Academy of Engineering Innovative Students Project Award for his Ph.D. thesis across all the institutes in India in 2019 and the IRD Student Start-up Award in 2017 in IIT Delhi during his doctoral studies. He also holds the Position of Secretary for the IEEE Young Professionals Affinity Group in Denmark Section.

Meysam Yaribeygi received the B.Sc. degree in electrical engineering from the University of Kurdistan, Sanandaj, Iran, in 2015 and the M.Sc. degree in electrical engineering from the K.N. Toosi University of Technology, Tehran, Iran, in 2017. He is currently a Graduate Research and Teaching Assistant with the Optical Communication Network Lab, K.N. Toosi University of Technology. He is also a Research Engineer with the SINA Innovative Communications Systems, Tehran, Iran. His research interests include optical network control plane and resource allocation, optimization, programable networked microgrids, and software-defined networking.

Hassan Bevrani (Senior Member, IEEE) received the Ph.D. degree in electrical engineering from Osaka University, Suita, Japan, in 2004. He is currently a Full Professor and Program Leader with Smart/Micro Grids Research Center University of Kurdistan (UOK), Sanandaj, Iran. From 2016 to 2019, he was the UOK Vice Chancellor for Research and Technology. Over the years, he has was a Senior Research Fellow and a Visiting Professor with Osaka University, Kumamoto University, Kumamoto, Japan, Queensland University of Technology, Brisbane, QLD, Australia, Kyushu Institute of Technology, Fukuoka, Japan, Centrale Lille, Villeneuve-d'Ascq, France, and Technical University of Berlin, Berlin, Germany. He is currently a Visiting Professor with Osaka University. He is the author of six international books, 15 book chapters, and more than 300 journal or conference papers. His current research interests include smart grid operation and control, power systems stability and optimization, microgrid dynamics and control, andintelligent or robust control applications in power electric industry.

Tomislav Dragicevic (Senior Member, IEEE) received the M.Sc. and industrial Ph.D. degrees in electrical engineering from the Faculty of Electrical Engineering, Zagreb, Croatia, in 2009 and 2013, respectively. From 2013 to 2016, he was a Postdoctoral Research Associate with Aalborg University, Aalborg, Denmark, where he was an Associate Professor from 2016 to 2020. Since 2020, he has been a Professor with the Technical University of Denmark, Kongens Lyngby, Denmark. He was a Guest Professor stay with Nottingham University, Nottingham, U.K., during the Spring or Summer of 2018. He has authored or coauthored more than 200 technical articles (more than 100 of them are published in international journals, mostly in IEEE), eight book chapters, and a book in his research fields. His main research interests include the design and control of microgrids, and the application of advanced modeling and control concepts to power electronic systems. He was the recipient of the Koncar Prize for the Best Industrial Ph.D. Thesis in Croatia and the Robert Mayer Energy Conservation Award. He was the Winner of Alexander van Humboldt Fellowship for experienced researchers. He is currently an Associate Editor for the IEEE TRANSACTIONS ON INDUSTRIAL ELECTRONICS, IEEE TRANSACTIONS ON POWER ELECTRONICS, IEEE JOURNAL OF EMERGING AND SELECTED TOPICS IN POWER ELECTRONICS, and *IEEE Industrial Electronics Magazine*.

Authorized licensed use limited to: East Carolina University. Downloaded on June 18,2021 at 00:44:42 UTC from IEEE Xplore. Restrictions apply.